

Comprehensive Stator Turns Fault and Iron Loss in Three Phase Induction Motors Using Finite Element Method

Ahcène Bouzida^{#1-2}, Omar Touhami^{#2}, Radia Abdelli^{*3}

^{#1} M'hamed Bougara University-Boumerdes, Algeria

^{#2} Ecole Nationale Polytechnique, Algiers

¹bouzida.umbb@gmail.com

^{*3} University TARGA OUZEMOUR (TAGHZOUIT) Béjaia -6000-Algérie

³abdelli_radia@yahoo.fr

Abstract— Stator short circuit fault in the three-phase squirrel-cage induction motor is analyzed by time stepping finite element method using different characteristics and iron loss computation under no load condition. Generally, the stator short circuit fault reduces the ability of produce a balanced electrical field, causing vibration increase on the machine, and consequently, isolation degradation and motor bearings failure. This study uses 2-D finite element (FE) models for detailed field analysis and considers different saturation levels. The use of advanced CAD package like FLUX2D, MAXWELL2D or FEM allows the computing of the iron losses in the different regions. Stator current frequency spectrum over low frequencies for the different cases is described. The simulation of the proposed model allows extraction of the flux density, inductances, currents, torque, forces, iron losses... etc and their values are compared under healthy and faulty conditions.

Keywords—Induction Motor, Iron Loss, Stator fault, Finite element method, Modeling, Simulation.

I. INTRODUCTION

Three phase induction machines is recognized that a variety of faults can occur in these machines as rotor fault, stator inter-turn fault, eccentricity and others mechanical faults. Hence early detection of such faults are very essential for the protection of induction motors. A sudden motor failure may reduce productivity and may be catastrophic in an industrial system if undetected in the necessary time. The interior faults of induction motor accounts for more than 70 % in proportion of induction motor failures. Interior faults include stator and rotor faults of induction motors. Rotor faults are related to broken bars. Rotor failures are caused by a combination of various stresses that act on the rotor and these stresses can be identified as electromagnetic, thermal, dynamic,...

This steady focuses on the induction motors under stator short circuit faults using the finite element method to flow the dynamic behavior by monitoring the dynamic

characteristics under no load condition. Whoever the induction machine simulation has also performed to understand the imbalance caused by the stator short circuit by avoiding the effect of other type of faults rated to load. The use of the winding function allows to calculate the different inductances and mutual inductances if the windings become asymmetrical while basing on the calculation of the equivalent resistances. These approaches are based on simplifying assumptions which ignore many phenomena such as the magnetic saturation, the skin effect, the eddy currents and the non sinusoidal distribution of FMM in the air-gap; thus results a simulation whose don't describe the real behavior of the machine. The study of the stator short circuit by using the finite element method [4-5-6] makes simulation more significant and the results are closed to the practical results.

The transient analysis was done using coupled electric circuit with 2D finite element electromagnetic field analysis for healthy and defective induction machine. The designed geometric dimension is modeled in the finite element domain and transient performances are predicted at the starting of motor with no load. Many test have been examined for inter turns faults [8-9] .

II. MODELING OF INDUCTION MACHINE USING FINITE ELEMENT METHOD (FEM)

The software FLUX2D [8] is chosen to simulate the proposed model of the induction machine and the magnetic transitory formulation is included, which solves the problem in discrete time points. The geometry of the materials and the development of the winding were obtained by fragmenting a real motor, in which field test were performed. Figures 1 shows the machine geometry entirely and meshing, in which stator and rotor core regions, and squirrel's cage bars are shown. The computing of iron loss is enabled for the stator and rotor cores.

Figure 2 shows electrical circuit used in the healthy motor simulations. This circuit is divided in three parts: external sources, stator circuit and the squirrel cage. To make

the different simulations of the short-circuit turns motor, the winding are divided in many parts in the faulty cases.

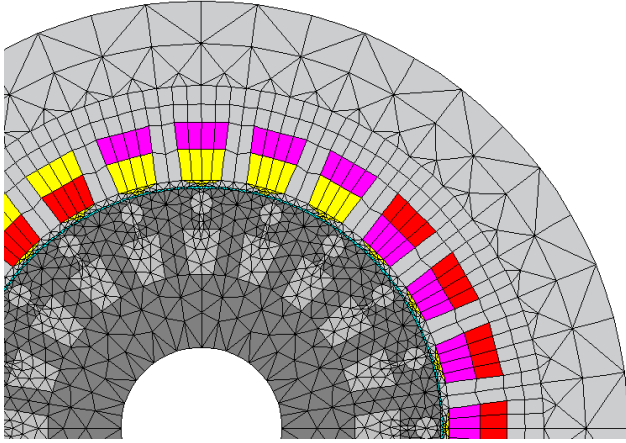


Fig. 1: Induction machine regions mesh

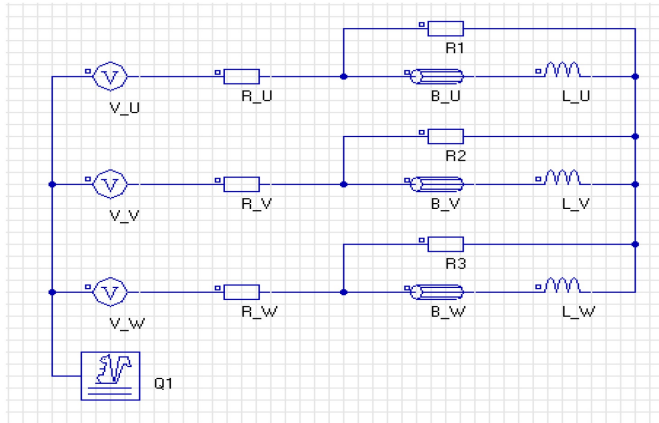


Fig. 2: Electrical Circuit coupling

III. IRON LOSS CALCULATION

The study into magneto-transient is appropriate particularly well for our need. The coupling of our magnetic diagram to an electrical circuit and the presence of a tread in the air-gap make it possible to follow the dynamic behavior of the machine and the studied model allows to computing the iron losses in each region. The magneto-transient simulation using the software Flux2D is based on the resolution of the following equation:

$$\sigma_e \frac{d\vec{A}}{dt} + \text{rot} \left(\frac{1}{\mu \text{rot}(\vec{A})} \right) = J + \text{rot}(\vec{H})$$

Where:

A : Magnetic potential (Weber/m)

J : Density of current (A/m)
 μ : Magnetic permeability (H/m)
 H : Magnetic field (A/m)
 σ_e : Electric conductivity (1/m)
 t : Time(s)

Iron loss in magnetic material, subjected to an alternating magnetic field in the range of low and medium frequencies, is the result of eddy currents generated in the material, which is characterized by its specific conductivity. Recently, we have presented a model to the energy loss in magnetic material basing on scaling theory.

Nowadays, a number of phenomena occurring in different spatial scales in the material is recognized, which can be accounted for the source of induced eddy currents. Eddy currents may be induced on micro-scale due to the Barkhausen jumps, which results in a theoretical dependence $P_{phy} \propto f B_m^\alpha$, where f is frequency of magnetizing field, B_m is maximum magnetic induction and α is constant, unique for a specific material, on the intermediate scale i.e. around moving domain walls $P_{ext} \propto (f B_m)^{3/2}$, as well as on macro-scale, covering the whole material volume $P_{class} \propto (f B_m)^2$ [10-11]. The contemporary approach to energy loss phenomenon in magnetic materials assumes that the total loss P_{tot} is the sum of described above contributions:

$$P_{tot} = C_1 f B_m^\alpha + C_2 (f B_m)^{3/2} + C_3 (f B_m)^2$$

where C_1, C_2, C_3 are constants. The approach to iron loss, which assumes their additive character, allows for their separation and consequently for the independent analysis of the obtained components in different scales. However, the results obtained in the case of modern materials of amorphous and microcrystalline structure reveal discrepancies between the theoretical and experimental values.

The iron losses can be calculated in a magnetic area during the simulation process. They include the hysteresis losses, the traditional losses and the excess losses [10-11]: In magneto-dynamic the losses is given by:

$$dP_{tot} = k_h B_m^2 \cdot f + \pi^2 \frac{\sigma d^2}{6} (B_m \cdot f)^2 + k_e (B_m \cdot f)^{3/2} \times 8,67$$

in periodic mode (magneto-transient during complete period):

$$\frac{1}{T} \int_0^T d P_{tot}(t) dt = k_h B_m^2 f k_f + \frac{1}{T} \int_0^T \left[\sigma \frac{d^2}{12} \left(\frac{dB}{dt}(dt) \right)^2 + k_e \left(\frac{dB}{dt}(dt) \right)^{3/2} \right] k_f dt$$

Where B_m is maximum magnetic induction at the considered node, f is frequency of magnetizing field, d the thickness

magnetic sheet, k_h the hysteresis loss coefficient and k_e the excess losses coefficient.

The numerical simulations in this paper refer to following induction motor specifications:

TABLE I: Induction Motor specifications

| | |
|---------------------------|------------|
| Rated power | 7,5 Kw |
| Rated Voltage | 380 V |
| Rated line current | 8.83 A |
| Rated speed | 2850 tr/mn |
| Coupling | Star |
| Poles | 2 |

The machine was simulated for 3 cases:

- ✓ Case A: Healthy Machine and machines
- ✓ Case B: Machine With 10 short-circuit turns
- ✓ Case C: Machine With 50 short-circuit turns

IV. RESULTS OF SIMULATION

By the computation of the electromagnetic field using Finite element analysis, the machine inductance and back EMFs can be obtained. The parameters obtained from the FEM analysis contain the information of the fault location and severity. The flux distribution for the different simulation cases are shown in the Figures 3.

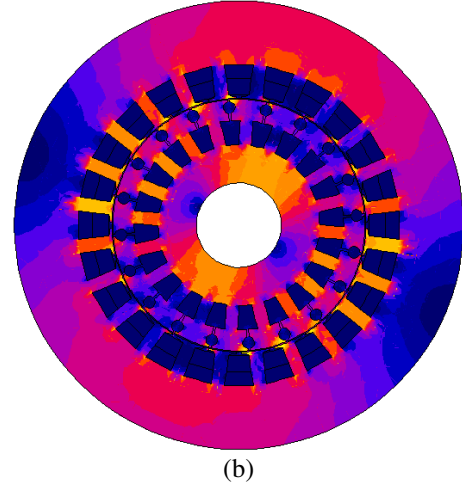
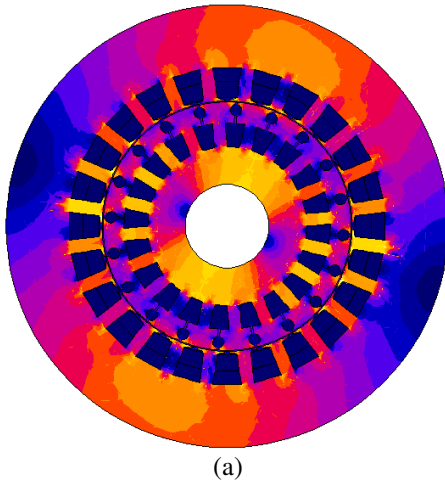


Fig. 3: Flux distribution under no load condition
 (a) healthy machine, (b) machine with 50 shorted turns

The numerical results corresponding to a magnetic flux analysis of the 2D electromagnetic field-circuit problem associated to the induction motor, figures, number of short-circuited turns determines a decrease of the distribution of the field density. Another effect of this type of fault, consists in an important increase with the number short-circuit turns. Under the healthy conditions, the distribution of magnetic field is symmetrical, while the magnetic field distribution is unsymmetrical in the case of short-circuit turns faults.

A. STATOR CURRENT ANALYSIS

The stator current is the most useful signature used to monitoring the induction machines under faulty conditions. Whoever the calculated stator current waveforms for different studied cases are shown Figure 4. The figure 4 shows clearly the increasing in the current amplitude for the defective cases.

The analysis of the stator current using the MCSA is also used as a powerful tool for the detection of the default in the induction machines. In this part the power spectral density has been used to extract the frequency components rated to the faults. The figure 5 presents the different normalized PSD waveforms of the stator current under no load condition.

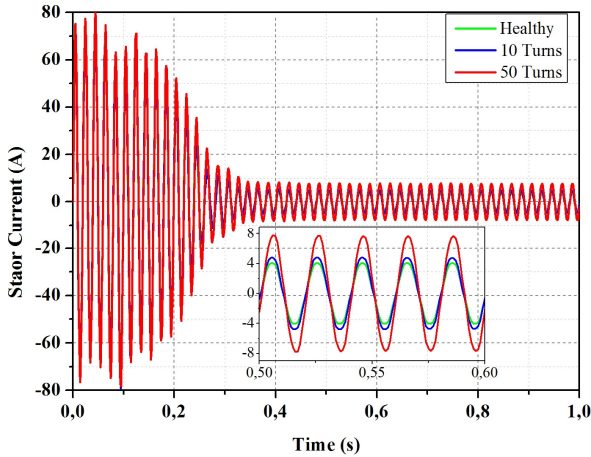


Fig. 4: Stator current under no load condition

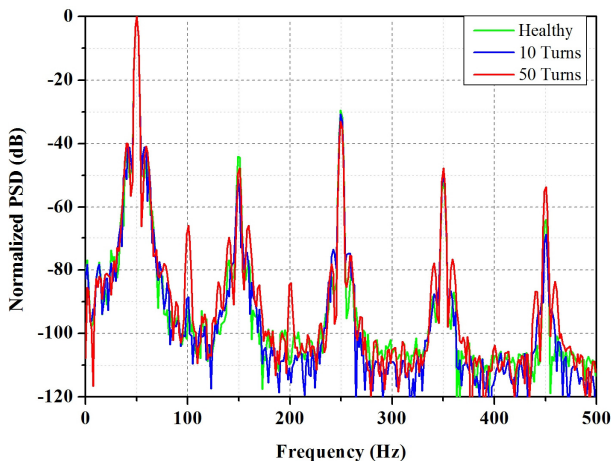


Fig. 5: Normalized PSD of the stator Current

It is observed that the amplitude of the frequency components located at $2f$ and $4f$ increase in the defective cases and, it is clear that the amplitude increases as the number of short-circuit turns increases.

B. IRON LOSS ANALYSIS

In this section, the simulation results for the Transient Analysis of three phase induction motor for healthy motor and faulty motor with 10 and 50 short-circuit turns under no load condition are presented and the iron loss are calculated on the different regions.

The figures 6, 7 et 8 show the iron losses for the stator core, rotor core and the total core losses for the three proposed simulation cases.

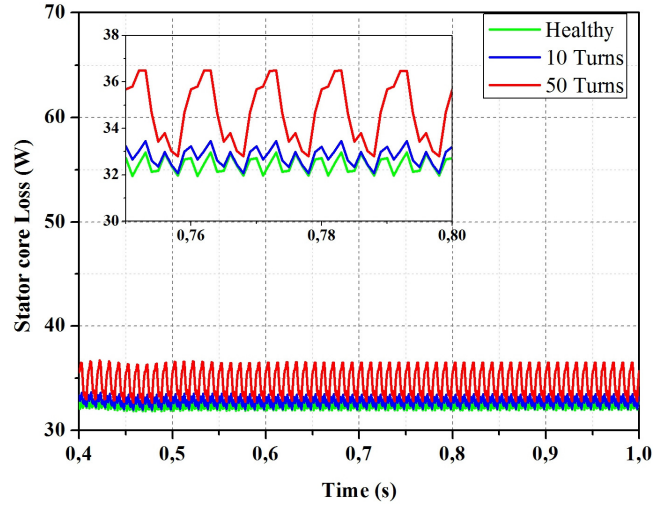


Fig. 6: Stator core iron loss

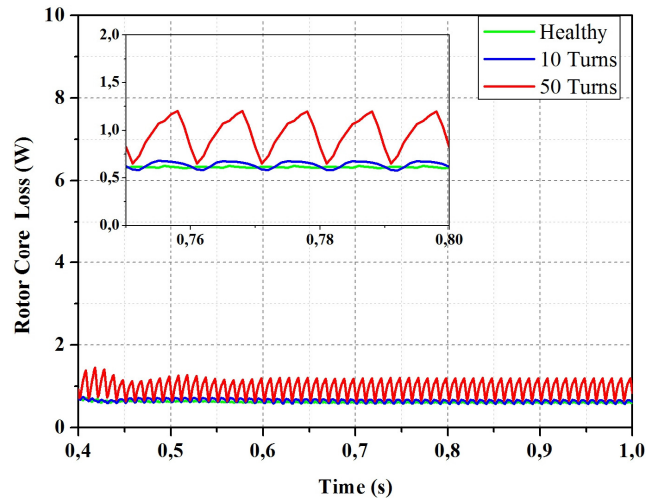


Fig. 7: Rotor core iron loss

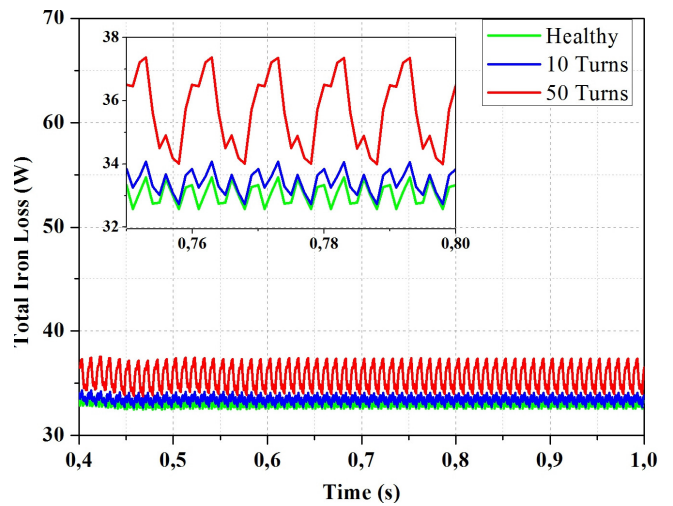


Fig. 8: Total iron losses

The computed losses for the different cases shows clearly show the effect of the short-circuit turns, The iron losses increase with the default degree in the stator and rotor cores. On the other hand this simulation has been performed under no load condition, for the rated load the increasing of total iron losses becomes more and more important and the machine efficiency will be affected.

IV. CONCLUSION

FE analysis is used for describe the Induction Machine with short-circuit turns fault and the computing of the iron losses under no load condition. The different performances can be determined when the simulation is done. The proposed model is used for studying the machine behavior under fault condition and the FEM model of the Induction machine has enables to calculate several parameters (Flux, Torque, Forces, losses ...etc). The comparison between the various parameters obtained for the healthy and defective machine has been performed and we note that this method of analysis clearly shows the effect of the short-circuit turns on the behavior of the machine and.

REFERENCES

- [1] D. Diaz, M. C. Amaya, A. Paz. "Inter-turn Short-circuit Analysis in an Induction Machine by Finite Elements Method and Field Tests" XXth, International Conference on Electrical Machines (ICEM), IEEE 2012, Page(s):1757 - 1763.
- [2] J. Seshadrinath, B. Singh, K. Panigrahi. "Single-Turn Fault Detection in Induction Machine Using Complex-Wavelet-Based Method". IEEE Transactions on industry applications, VOL. 48, 2012, Page(s):1846-1854.
- [3] M. Arkan, D. Kostic-Perovi, K. P.J. Unsworth. "Modelling and simulation of induction motors with inter-turn faults for diagnostics-Based Method". Electric Power Systems Research, VOL. 75, 2005, Page(s):57-66.
- [4] Ebrahimi, B.M. , Akin, B. , Toliyat, H.A. "Finite-Element Transient Analysis of Induction Motors Under Mixed Eccentricity Fault ". IEEE Transactions on Magnetics, VOL. 44, 2008 , Page(s):66-74.
- [5] Nagarajan S. and RamaReddy S. "Diagnosis And Characterization Of Effects Of Broken Bars In Three Phase Squirrel Cage Induction Motor Using Finite Element Method". ARPN Journal of Engineering and Applied Sciences, VOL. 7, Sep 2012 , Page(s):1170-1179.
- [6] B.A.T. Iamamura, Y. Le Menach, A. Tounzi, N. Sadowski, and E. Guillot; "Study of Static and Dynamic Eccentricities of a Synchronous Generator Using 3-D FEM". IEEE Transactions on Magnetics, VOL. 46, AUG 2010 , Page(s):3516-3519.
- [7] David G. Dorrell and Min-Fu Hsieh; "Calculation of Radial Forces in Cage Induction Motors at Start?The Effect of Rotor Differential". IEEE Transactions on Magnetics, VOL. 46, AUG 2010 , Page(s):3029-3032.
- [8] Salah Eddine Zouzou, Samia Khelif, Noura Halem and M. Sahraoui, "Analysis of Induction Motor with broken rotor bars Using Finite Element Method". International Conference on Electric Power and Energy Conversion Systems (EPECS), 2011, Page(s):1-5.
- [9] Nistor, C.G. ; Plesa, O.I. ; Scutaru, G. ; Peter, I. ; Ionescu, R.M. "Numerical modeling of magnetic noise for three phase asynchronous motors through the software Flux 2D ".International Conference on Applied and Theoretical Electricity (ICATE), 2012, Page(s):1-4.
- [10] Bashir Mahdi Ebrahimi, Amir Masoud Takbash, and Jawad Faiz" Losses Calculation in Line-Start and Inverter-Fed Induction Motors Under Broken Bar Fault". IEEE TRANSACTIONS ON INSTRUMENTATION AND MEASUREMENT, VOL. 62, NO. 1, JANUARY 2013. pp. 140-152.
- [11] J. F. Bangura, and N. A. Demerdash, " Effects of Broken Bars/End-Ring Connectors and Airgap Eccentricities on Ohmic and Core Losses of Induction Motors in ASD's Using a Coupled Finite Element-State Space Method", IEEE TRANSACTIONS ON ENERGY CONVERSION, VOL. 15, NO. 1, 2000, pp.40-47.